Laminar-Turbulent Transition: Calculation of Minimum Critical Reynolds Number in Channel Flow

Hidesada Kanda

University of Aizu, Aizu-Wakamatsu, Fukushima 965-8580, Japan
kanda@u-aizu.ac.jp

Abstract

A conceptual model has been constructed for the problem of determining a critical Reynolds number (Rc) for laminar-turbulent transition in pipe and channel flows. For pipe flow, the minimum critical Reynolds number $Rc(min)$ of approximately 2040 was obtained. In order to prove the validity of the model, another verification is required. Thus, for channel flow, results of previous investigations were studied, focusing on experimental data on Rc, the entrance length, and the transition length. Consequently, the model was confirmed and an experimental value of $Rc(min)$ in the neighborhood of 1300 was found to exist, based on the channel height and average velocity. *In this study, for channel flow, we obtained $Rc(min)$ of approximately 1230 when using $J0 = 101$ grid points in the normal or y-direction, and 910 when $J0 = 51$.*

BD	bellmouth diameter
D	pipe diameter
h	one-half of channel height
H	channel height $= 2h$; enthalpy
i	grid point in x-direction
$I0$	maximum number of grid points in x-direction
j	grid point in y-direction
$J0$	maximum number of grid points in y-direction
$K(X)$	excess pressure drop
KE	increase in kinetic energy
Le	dimensionless entrance length $= x'_e/(HRe)$
NWS	normal wall strength
p	dimensionless pressure $= p'/(1/2 * \rho U^2)$
p'	pressure
p_c	pressure at centerline
p_w	pressure at wall
PW	power done by NWS
Rc	critical Reynolds number for transition
$Rc1$	Rc from laminar to turbulent flow
$Rc2$	Rc from turbulent to laminar flow
$Rc(min)$	minimum Rc
Re	Reynolds number $= UH/\nu$
t	dimensionless time $= (U/H)t'$

t'	time
u	dimensionless x component of velocity $= u'/U$
U	average velocity in x-direction; internal energy
u'	x component of velocity
v	dimensionless y component of velocity $= v'/U$
V	velocity vector $= (u, v)$; volume
v'	y component of velocity
x	dimensionless coordinate along channel $= x'/H$
x'	coordinate along channel
x'_e	entrance length
X	dimensionless x-coordinate $= x'/(HRe) = x/Re$
y	dimensionless coordinate across channel $= y'/H$
y'	coordinate across channel
ν	kinematic viscosity
ψ	dimensionless stream function $= \psi'/(UH)$
ψ'	stream function
ω	dimensionless vorticity $= (H/U)\omega'$
ω'	vorticity

1 Introduction

1.1 Background and objectives

In 1883, Reynolds first observed two different kinds of critical values (Rc) for laminar-turbulent transition in pipe flows: (i) $Rc = 12{,}830$ determined by the color-dye method and (ii) $Rc = 2030$ determined by the pressure loss method [1, 2]. Thus, the Reynolds's problem is defined as the theoretical obtainment of $Rc = 12{,}830$ and $Rc = 2030$ for pipe flows. The value of 2030 is called the minimum Rc, or $Rc(min)$. To date, attempts to solve this problem have been undertaken using the stability theory with the Orr-Sommerfeld equation and disturbances. However, $Rc(min)$ of approximately 2000 has not yet been obtained. For flow in the entrance region, Tatsumi [3] obtained $Rc = 19{,}400$ and Huang and Chen [4] obtained $Rc = 39{,}800$ and $39{,}560$ due to axisymmetric and non-axisymmetric disturbances, respectively.

Reynolds observed that the transition for Rc of 12,830 occurs near the pipe inlet, or in the entrance region. Generally, thus far, three major variables have been studied in the entrance region [5a]: (i) the velocity distribution at any section, (ii) the entrance length (Le), and (iii) the pressure difference between any two sections and the excess pressure drop (K(∞)). In dimensionless X coordinates, the results of the velocity distribution, Le, and K(∞) are approximately constant regardless of Reynolds numbers (Re) when $Re > 500$ [6], i.e., these variables are not functions of Re above 500. However, since the transition occurs in the entrance region, we must find a variable which varies inversely with Re around $Rc(min)$. It is found to be the normal wall strength (NWS, see Eq. (15)).

On the basis of the above discussion and the results of many previous experimental investigations, we developed a transition model (see next subsection) and obtained $Rc(min)$
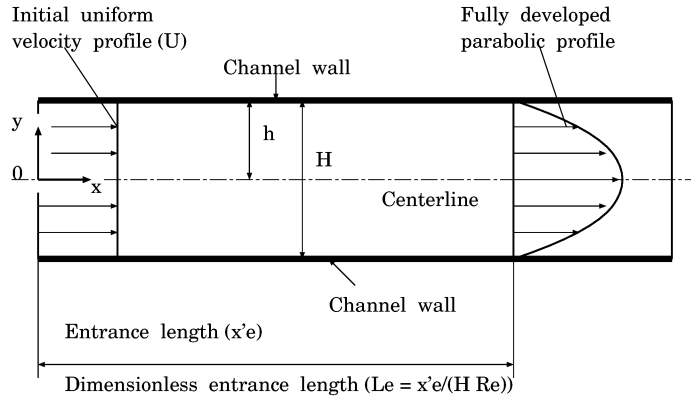
Figure 1: Velocity development in the entrance region.

= 2040 using the axial grid points $J0 = 101$, and $Rc(min) = 2630$ at $J0 = 51$ [7, 8]. The purpose of the present study is to obtain $Rc(min)$ numerically for channel flow, which satisfies the experimental minimum value in the neighborhood of 1300, and thus to verify the model of the occurrence of the transition.

Although many investigations were carried out for channel flow, there are few implicit solutions available in the normal or y-direction [9, 10]. For the experimental $Rc(min)$ value in channel flow, Davies and White [11] observed a $Rc(min)$ value of 1440 when using a straight channel of rectangular cross section with the aspect ratio of 37 through 165. $Rc(min) = 1440$ was obtained in the fully developed region, while the $Rc(min)$ value in the entrance region was not clear. Patel and Head [12] carried out experiments in a straight rectangular channel 1/4 in. high and 12 in. wide in the fully developed region. The aspect ratio of 48 was considered sufficient to assume the flow to be two-dimensional. Patel and Head stated that the value of approximately 1300 may be acceptable as the lower or minimum critical value for channel flow.

On the other hand, the theoretical $Rc(min)$ calculated using stability theory is about 7700 [13].

1.2   Transition model

The following outline of the model is considered for pipe flow. Similarly, this model is applicable to channel flow since both flows are internal flow. Only critical values for $Rc(min)$ are different between pipe and channel flows.
(1) Four laminar-turbulent transition types:
Figure 1 shows the entrance region between parallel plates at $y = \pm h$ in two dimensions. At the inlet $x = 0$, let us assume that the fluid enters the channel with a flat axial velocity profile U across parallel plates, and that there is no velocity component in the y-direction. In the entrance region, the velocity distribution progresses from uniform at the inlet to parabolic downstream beyond Le. The region beyond Le is called the fully developed region. Reynolds stated that there are two critical values for velocity in a pipe: one at which steady motion

3

Table 1: Four types of laminar-turbulent transition.

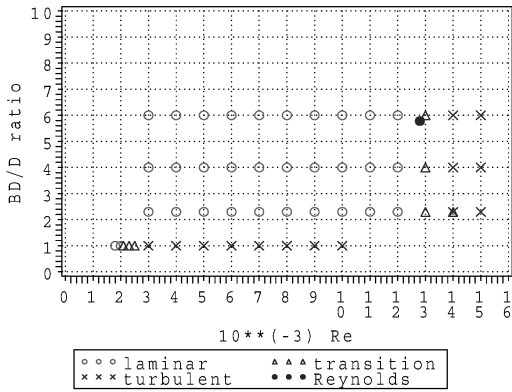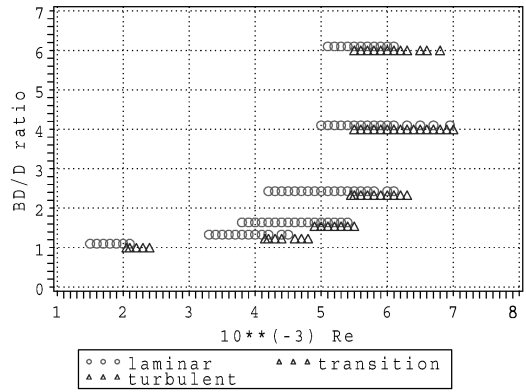| Transition type	Entrance region	Fully developed region
Laminar to turbulent	$Rc1$	$Rc3$
	(color-dye method)	
Turbulent to laminar	$Rc2$	$Rc4$
	(pressure loss method)	(pressure loss method)

Figure 2: Flow state for $Rc1$ vs BD/D.

Figure 3: Flow state for $Rc2$ vs BD/D.

changes into eddies, and another at which eddies change into steady motion. We also recognized two types of transition in the entrance region: $Rc1$ is Rc for transition from laminar to turbulent flow and $Rc2$ is another Rc for transition from turbulent to laminar flow [14]. Accordingly, the laminar-turbulent transition is classified into four types according to the distance from the inlet and Rc, as shown in Table 1. Reynolds' color-dye method is applicable for $Rc1$ and his pressure loss method for $Rc2$ and $Rc4$, although $Rc2$ and $Rc4$ might be for the same transition phenomenon.

(2) Effects of entrance shape on Rc:

Prandtl and Tietjens state that in order to obtain a high Rc, it is essential to round off the entrance of the pipe [15]. Figures 2 and 3 show the experimental results for $Rc1$ and $Rc2$, respectively [14]. Values of $Rc1$ and $Rc2$ increase as the contraction ratio of the bellmouth (BD) to pipe diameter (D) increases. It is clear that each entrance shape has a maximum value for $Rc1$ and a minimum value for $Rc2$: $Rc1(BD/D, max)$ and $Rc2(BD/D, min)$. $Rc1(BD/D \geq 2.33, max)$ approaches a constant of approximately 13,000, above which the flow state is turbulent. Similarly, $Rc2(BD/D \geq 2.33, min)$ approaches a constant of approximately 5500, below which the flow state is laminar. Generally, $Rc2(min) \leq Rc1(max)$ and the two lines for $Rc1(max)$ and $Rc2(min)$ form a hysteresis curve like that in an electromagnetic field.

(3) Minimum critical value, $Rc(min)$:

From the experimental results [14], $Rc(min)$ is obtained when the contraction ratio BD/D

at the inlet is minimum or one, i.e., without any bellmouth entrance. Then, the values of both $Rc1(max)$ and $Rc2(min)$ become $Rc(min)$ of approximately 2000. Concerning the effects of the sharp corners of a straight channel on Rc, Patel and Head stated that "initially the channel was connected directly to the setting box and it was thought that the sharp corners at the inlet would provide sufficiently disturbed conditions. However, to make quite sure that the flow was fully turbulent, a 1/8 in. diameter wire was later fitted across the inlet, and it was found that this did not alter the results in any way" [12]. For pipe flow,

$$\lim_{BD/D \to 1} \text{Rc(min)} \ = \ Rc2(min) \ \approx \ Rc1(max) \ \approx \ 2000. \tag{1}$$

(4) Normal wall strength (NWS):
NWS is defined as the radial component of the curl of vorticity multiplied by ($2/Re$) (see Eq. (15)). Note that NWS varies approximately inversely with Re and the boundary-layer assumption neglects NWS.

$$NWS \ \equiv \ \frac{2}{Re} \left[\nabla \times \omega \right]_r \Big|_{r=R} \tag{2}$$

(5) Increase in kinetic energy (KE):
The magnitude of the increase in kinetic energy in the entrance region is named KE, although its physical unit is power, not energy (see Eq. (43)). Note that KE is a constant regardless of Re, unlike NWS.
(6) The judgement condition for the occurrence of the transition depends on whether the power (PW) done by NWS is higher or lower than the required acceleration power (KE) for fully developed flow.
    (i) When $PW < KE$, transition takes place.
    (ii) When $PW \geq KE$, flow is stable.
(7) Internal flows:
When considering the transition, internal flows such as pipe flow and channel flow must be separated from external flows, such as flow on a flat plate, since the external flows do not reach any fully developed state. The laminar-turbulent transition is determined by whether the flow reaches a fully developed state. For external flows, the transition occurs necessarily after some distance from the inlet. For flow on a flat plate, Rivas and Shapiro [16] state that the length Reynolds number of transition ($Rx = Ux'/\nu$) is of the order of 500,000.
(8) Natural calm conditions:
Transition occurs in the entrance region under the conditions of natural calm disturbances. Artificial disturbances are not considered.

A few fundamental points, however, still remain unsolved in the model.
(1) It is insufficient for predicting the transition length, which is the distance between the inlet and the point where the transition to turbulence occurs.
(2) It is insufficient for quantitatively explaining the periodical generation and decay of "puffs and slugs" [17]. NWS might be a force that controls the puffs and slugs.

2 Calculated results

2.1 Governing equations

First, let us consider dimensionless variables. All lengths and velocities in the problem are normalized by the channel height $H(= 2h)$ and the mean velocity U, respectively. The pressure is normalized by $(1/2)\rho U^2$, not ρU^2. The Reynolds number is based on the channel height H and the mean velocity U. Note that x is used for calculation and $X(= x/Re)$ for presentation in figures and tables.

The equations that govern the incompressible laminar flow are the vorticity transport equation,

$$\frac{\partial \omega}{\partial t} + \frac{\partial \psi}{\partial y}\frac{\partial \omega}{\partial x} - \frac{\partial \psi}{\partial x}\frac{\partial \omega}{\partial y} = \frac{1}{Re}\nabla^2\omega, \tag{3}$$

and Poisson's equation for the stream function:

$$\nabla^2\psi = -\omega. \tag{4}$$

The relationships between the stream function and velocity are defined as

$$u = \frac{\partial \psi}{\partial y}, \qquad v = -\frac{\partial \psi}{\partial x}. \tag{5}$$

In a two-dimensional flow field, only the z component of vorticity, ω_z, is effective; thus, ω denotes ω_z in this study.

$$\omega = \omega_z = [\nabla \times V]_z = \frac{\partial v}{\partial x} - \frac{\partial u}{\partial y} \tag{6}$$

The $\psi - \omega$ solution does not give any information regarding the pressure field. The pressure can be calculated using the Navier-Stokes equations in a steady state [18a]; the pressure distribution for the x derivative is

$$\frac{\partial p}{\partial x} = -2\left(u\frac{\partial u}{\partial x} + v\frac{\partial u}{\partial y}\right) + \frac{2}{Re}\nabla^2 u, \tag{7}$$

and that for the y derivative is

$$\frac{\partial p}{\partial y} = -2\left(u\frac{\partial v}{\partial x} + v\frac{\partial v}{\partial y}\right) + \frac{2}{Re}\nabla^2 v. \tag{8}$$

Since u and v are known at every point from Eq. (5), the derivatives on the right-hand sides of Eqs. (7) and (8) can be obtained. Hence, note that the results of Eq. (7) must satisfy the results of Eq. (8). Thus, a smooth pressure distribution which satisfies both Eqs. (7) and (8) is calculated using Poisson's equation [19],

$$\nabla^2 p = -4\left[(\frac{\partial v}{\partial x})(\frac{\partial u}{\partial y}) - (\frac{\partial u}{\partial x})(\frac{\partial v}{\partial y})\right]. \tag{9}$$

For the calculation of pressure distribution, it is important to make no assumptions. Accordingly, the vorticity transport equation is first solved and then the pressure distribution equation is solved without any assumptions made for pressure distribution. In this study, initial values are given using Eq. (7), and then Eq. (9) is used to obtain better solutions.

2.2 Le and excess pressure drop $K(\infty)$

The entrance length Le is defined by Eq. (10), as the length required for the centerline velocity to reach 98%, 99%, and 99.9% of its fully developed value.

$$Le \;=\; \frac{x'_e}{HRe} \tag{10}$$

For the fully developed flow where $\partial p/\partial y = 0$, the pressure gradient at the centerline [20] is given by

$$-\frac{dp}{dx} \;=\; \frac{24}{Re}. \tag{11}$$

The total pressure drop from the channel inlet is expressed as the sum of the pressure drop that would occur if the flow were fully developed plus the excess pressure drop $K(X)$ to account for the developing region.

$$p(0) - p(X) \;=\; 24X \;+\; K(X) \tag{12}$$

Generally, Le and $K(\infty)$ at $X \geq Le$ is calculated to verify the accuracy of the calculated results by comparison with other previous results.

2.3 Normal wall strength (NWS)

We consider what accelerates the fluid particles in the central core. The dimensionless N-S equation in vector form [5b] is written as

$$\frac{\partial V}{\partial t} - V \times \omega \;=\; -\,grad\Big(\frac{p}{2} + \frac{V^2}{2}\Big) - \frac{1}{Re}\nabla \times \omega. \tag{13}$$

Since V = 0 at the wall, Eq. (13) at the wall decreases to

$$\frac{2}{Re}\nabla \times \omega\Big|_{y=h} \;=\; -\,grad(p)\big|_{y=h}\,. \tag{14}$$

The normal component of Eq. (14) is called the normal wall strength (NWS), which is expressed nondimensionally as

$$NWS \equiv \frac{2}{Re}[\nabla \times \omega]_y\Big|_{y=h} = -\frac{2}{Re}\frac{\partial \omega}{\partial x}\Big|_{y=h} = -\frac{\partial p}{\partial y}\Big|_{y=h} > 0. \tag{15}$$

The characteristics of NWS are as follows.
(i) It is clear from Eq. (15) that NWS causes the pressure gradient in the y-direction; in other words, the pressure gradient results from the curl of vorticity. NWS and the pressure gradient in the y-direction have the same magnitude at the wall, but are opposite in direction. Therefore, the direction of NWS is from the wall to the centerline.
(ii) NWS exists in the vicinity of the inlet where the vorticity gradient in the x-direction is large. NWS decreases inversely as Re increases.
(iii) When using the boundary-layer assumptions, NWS vanishes since the pressure gradient normal to the plates is always neglected in the assumptions.

Table 2: Mesh system, CPU times and PW.

Re	$I0/J0$	T-step	CPU	PW
500b	1001/51	2,500,000	425h 33m	0.7906
1000b	1001/51	3,400,000	450h 04m	0.4905
2000b	1001/51	2,000,000	101h 46m	0.2524
4000b	1001/51	2,900,000	408h 17m	0.1610
700	201/101	1,400,000	518h 43m	0.7824
1000c	1001/101	3,400,000	3,387h 28m	0.6167
1500	201/101	1,200,000	495h 45m	0.4582
2000	201/101	1,500,000	499h 50m	0.3660

2.4 Numerical method

For an unsteady problem, the vorticity transport equation, Eq. (3), in finite difference form can be solved in time using an explicit Gauss-Seidel iteration method. This computational scheme involves the forward-time centered-space (FTCS) method. The rectangular mesh system is listed in Table 2, where $I0$ and $J0$ are the maximum numbers of mesh points in the x- and y-directions, respectively. Table 2 also lists Re, the number of time steps needed to reach the steady state (T-step), CPU times, and the power PW calculated from Eq. (38).

The calculation algorithm is shown in Fig. 4, where n is the number of time steps and m is the iteration index. Steps 3, 4, and 8 are the Gauss-Seidel method. At the wall and the centerline, a three-point, one-sided approximation for derivatives is used to maintain second-order accuracy. The scheme thus has second-order accuracy in space variables, and first-order accuracy in time.

The explicit form for the vorticity transport equation is written as

$$\frac{\omega^{n+1} - \omega^n}{\Delta t} + \frac{\partial \psi^n}{\partial y} \frac{\partial \omega^n}{\partial x} - \frac{\partial \psi^n}{\partial x} \frac{\partial \omega^n}{\partial y} = \frac{1}{Re} \left(\frac{\partial^2 \omega^n}{\partial x^2} + \frac{\partial^2 \omega^n}{\partial y^2} \right). \tag{16}$$

The initial condition for the stream function is given by

$$\psi(i,j) = (j-1)\triangle y, \qquad 1 \le i \le I0, \quad 1 \le j \le J0. \tag{17}$$

Within the boundaries, the initial vorticity is obtained by solving Eq. (4). The velocities u and v are set using Eq. (5) whenever the stream function is newly calculated.

The following are the boundary conditions where $I1 = I0$ - 1, $I2 = I0$ - 2, $J1 = J0$ - 1, and $J2 = J0$ - 2.

(i) At the centerline: $\psi_{i,1} = 0$, $\quad \omega_{i,1} = 0$, $\qquad 1 \le i \le I1$.

(ii) At the inlet: $\psi_{1,j} = (j-1)\triangle y$, $\quad \omega_{1,j} = 0$, $\qquad 2 \le j \le J1$.

(iii) At the wall: $\psi_{i,J0} = J1\triangle y$, $\qquad 1 \le i \le I1$.

For vorticity, the boundary condition at no-slip walls is derived from Eq. (6). Using a three-point, one-sided approximation for derivatives, we obtain

$$\omega_{i,J0} = -\left.\frac{\partial u}{\partial y}\right|_{y=h} \approx -\frac{3u_{i,J0} - 4u_{i,J1} + u_{i,J2}}{2\triangle y} = \frac{4u_{i,J1} - u_{i,J2}}{2\triangle y}. \tag{18}$$
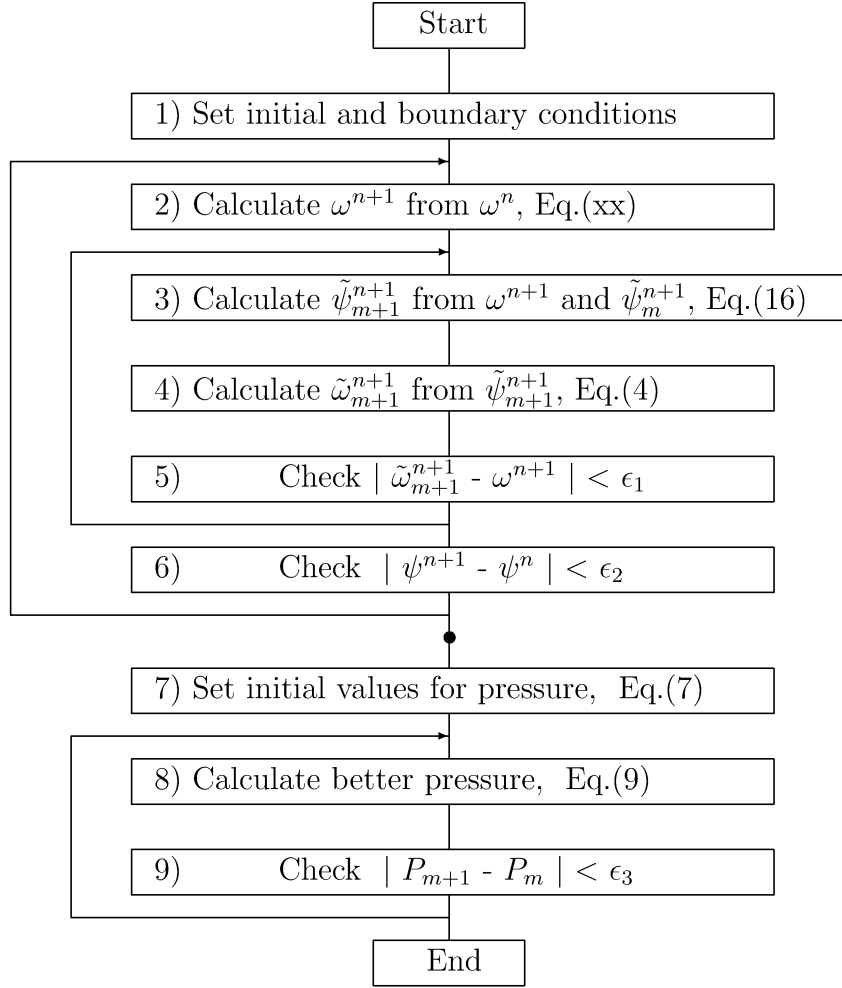
Figure 4: Flowchart for ψ -ω computer solution.

(iv) At the outlet, the linear extrapolation method is used: $\psi_{I0,j} = 2\psi_{I1,j} - \psi_{I2,j}, \quad \omega_{I0,j} = 2\omega_{I1,j} - \omega_{I2,j}$.

Then, we calculate a pressure distribution. The initial conditions are given by Eq. (7). The following are the boundary conditions for Poisson's equation for pressure.

(i) For the pressure at the centerline, we use the three-point finite difference form; since $\partial p/\partial y = 0$ at $y = 0$, $p_{i,1} = (4p_{i,2} - p_{i,3})/3$ with $1 \le i \le I0$.

(ii) The pressure at the channel inlet is given as zero without the leading edge: $p_{1,j} = 0, \quad 1 \le j \le J1$.

(iii) The pressure at the wall is derived from Eq. (15). For the leading edge with $i = 1$ and $j = J0$, using the three-point approximation for ω, the pressure gradient is expressed as

$$\frac{3P_{1,J0} - 4P_{1,J1} + P_{1,J2}}{2\triangle y} = \frac{2}{Re} \frac{-\omega_{3,J0} + 4\omega_{2,J0} - 3\omega_{1,J0}}{2\triangle x}. \tag{19}$$

Table 3: Dimensionless entrance length Le.

Re	98%	99%	99.9%	$K(\infty)$
500b	0.0330	0.0421	0.0756	0.6496
1000b	0.0331	0.0421	0.0748	0.6506
2000b	0.0330	0.0421	0.0758	0.6512
4000b	0.0329	0.0420	0.0746	0.6493
1000c	0.0330	0.0424	0.0732	0.6655
Bodoia and Osterle [21]	0.034	0.044	0.076	0.676
Kiya et al. [22]	0.0348	0.0445	-	0.666

For the wall with $2 \leq i \leq I1$ and $j = J0$,

$$\frac{3P_{i,J0} - 4P_{i,J1} + P_{i,J2}}{2\triangle y} = \frac{2}{Re}\frac{\omega_{i+1,J0} - \omega_{i-1,J0}}{2\triangle x}. \tag{20}$$

(iv) For the outflow boundary conditions, the linear extrapolation method is used: $P_{I0,j} = 2P_{I1,j} - P_{I2,j}, \quad 1 \leq j \leq J0$.

In this study, the dimensionless X-direction grid space is constant: $\triangle X = \triangle x/Re = 0.0001$. Accordingly, $\triangle x = 0.0001 * Re$ and the maximum X-distance is $0.0001 \times (I0 - 1) = 0.1$. The numerical calculations were carried out in 2002 on an NEC SX-4/128H4 supercomputer which has a peak performance of 2G-FLOPS/processor.

2.5 Calculated results

It is necessary to ascertain the accuracy of calculations. Table 3 lists the calculated values for Le and $K(\infty)$. The calculated results of this study agree well with the results of the previous investigations.

The transition occurs when X is less than 0.012-0.025 [23]. Accordingly, the pressure drop $\triangle p$ is calculated for $X \leq 0.02$, as shown in Figs. 5, 7, and 8, and for $X \leq 0.1$, as in Fig. 6. In Figs. 5 - 8, the black dots denote the pressure drop at the wall and the squares denote that at the centerline. The pressure p is 0 at the inlet. Since p is negative downstream, pressure drop $\triangle p$ in the x-direction is positive: $\triangle p = 0 - p$. The main conclusions for p and $\triangle p$ are as follows.

(i) The values of Le and $K(\infty)$ are approximately the same as listed in Table 3 at $Re \geq 500$.

(ii) There are large differences between pressures at the wall and at the centerline across the channel near the inlet. This difference becomes smaller as Re increases. Note again that the boundary-layer assumptions ignore this difference.
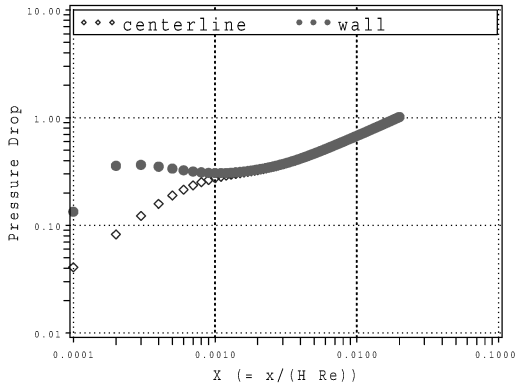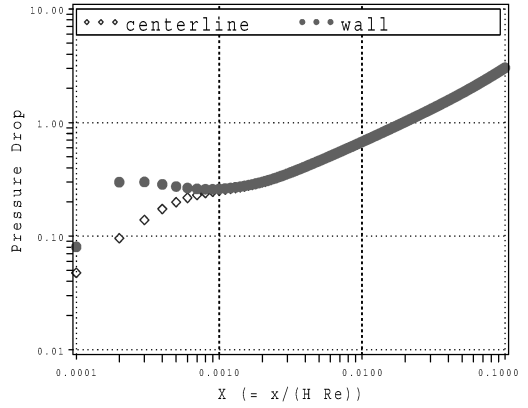
Figure 5: Normal pressure drop,
Re = 700c.

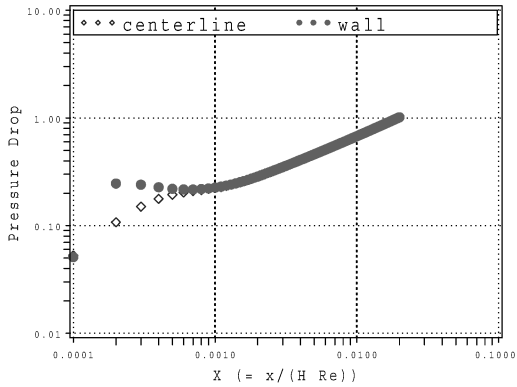Figure 6: Normal pressure drop,
Re = 1000c.
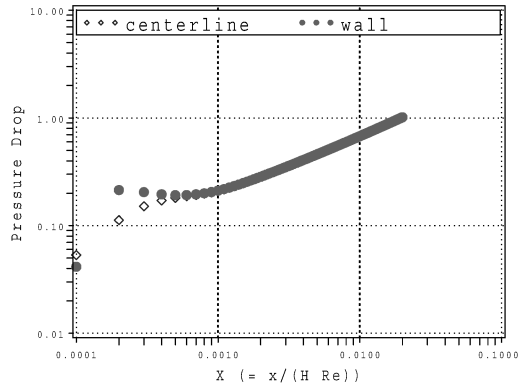

Figure 7: Normal pressure drop,
Re = 1500c.

Figure 8: Normal pressure drop,
Re = 2000c.

(iii) Hence, we consider the question: which is higher, pressure at the wall (p_w) or pressure at the centerline (p_c) in the y-direction? p_c is larger than p_w across the channel, indicating that the pressure distribution is contrary to Bernoulli's law, although the law does not apply to viscous flow. The calculated results verify Eq. (15).

3   Evaluation of pressure drop in normal direction

3.1   Verification of lower pressure at wall

At the wall, the vorticity is approximated from Eq. (18) as

$$\omega_{i,J0} = -\left.\frac{\partial u}{\partial y}\right|_{y=h} \approx \frac{4u_{i,J1} - u_{i,J2}}{2\triangle y}. \tag{21}$$

11

Near the wall, the x component of velocity, u, can be linearly approximated as

$$u_{i,J1} \approx \frac{(u_{i,J0} + u_{i,J2})}{2} = \frac{1}{2}u_{i,J2}. \tag{22}$$

From Eqs. (21) and (22), the vorticity at the wall is simply approximated as

$$\omega_{i,J0} = - \left.\frac{\partial u}{\partial y}\right|_{y=h} \approx \frac{u_{i,J1}}{\triangle y} > 0. \tag{23}$$

Substituting Eq. (23) into Eq. (15) gives

$$\left.\frac{\partial p}{\partial y}\right|_{y=h} = \left.\frac{2}{Re}\frac{\partial \omega_z}{\partial x}\right|_{y=h} = \left.\frac{2}{Re}\frac{\partial}{\partial x}(-\frac{\partial u}{\partial y})\right|_{y=h}$$

$$\approx \frac{2}{Re}\frac{\partial}{\partial x}(\frac{u_{i,J1}}{\triangle y}) = \frac{2}{Re}\frac{u_{i+1,J1} - u_{i-1,J1}}{2\triangle x\triangle y} \leq 0. \tag{24}$$

Hence, since $u_{i+1,J1} < u_{i-1,J1}$ in the entrance region, the normal pressure gradient at the wall becomes negative.

On the other hand, in the fully developed region, since $u_{i+1,J1} = u_{i-1,J1}$, the normal pressure gradient at the wall becomes 0, so that the pressure distribution is uniform in the y-direction, where the velocity distribution is given by

$$u(y) = \frac{3}{2}(1 - \frac{y^2}{h^2}). \tag{25}$$

For the value of the vorticity at the wall, differentiating Eq. (25) with respect to y gives

$$\omega|_{y=h} = - \left.\frac{\partial u}{\partial y}\right|_{y=h} = -\frac{3}{2}(-\frac{2h}{h^2}) = 3\frac{1}{h} = 6, \tag{26}$$

where the dimensionless value of h is 0.5. Thus, the value of ω decreases monotonically from a large positive value at the leading edge to 6 in the fully developed region. Hence, the positiveness of the vorticity in Eq. (23) is also verified.

3.2   Variation of enthalpy with pressure

Generally, power is defined as the inner product of force and velocity. If velocity u is in the x-direction, the power ($NWS \cdot u$) vanishes since NWS is perpendicular to u.

As shown in Figs. 5 - 8, however, there exist large pressure drops in the y-direction resulting from NWS. Hence, the amount of work done by NWS is considered using thermodynamics [24]. The variation of enthalpy H with pressure p, at a fixed temperature, can

be obtained from the definition $H = U + pV$, where U is internal energy and V is volume. For changes in H, we have

$$\triangle H \;=\; \triangle U \;+\; \triangle(pV). \tag{27}$$

For most solids and liquids, at a constant temperature, the total energy U does not change markedly with pressure. Since the change in volume can be neglected in comparison with the change in pressure, the change in enthalpy $\triangle H$ due to a change in pressure $\triangle p$ can be approximated by

$$Work\ done\ by\ NWS \;=\; \triangle H \;\approx\; V\triangle p \tag{28}$$

Equation (28) can be applied to an incompressible flow as well. The unit of $V\triangle p$ is expressed as

$$\left[m^3 \cdot kg\frac{m}{sec^2}\ \frac{1}{m^2} \;=\; kg\ \frac{m}{sec^2} \cdot m \right].$$

This unit, however, is equal to work in physics, and not to power such as the increase in kinetic energy per second. Accordingly, we must consider the duration in which the work given by Eq. (28) is done.

$$\left[power \;=\; \frac{energy}{time} \;=\; \frac{work}{time} \right]$$

3.3 Power PW done by NWS

The power done by NWS can be obtained by dividing the work by elapsed time. First, consider the volume size $V(i)$ which NWS affects. For the shaded space between $x(i)$ and $x(i+1)$ in the rectangular mesh system shown in Fig. 9, it is assumed that NWS has an effect on the volume in the range from $y(J1)$ to $y(j)$ in the y-direction. Since there are few differences in pressure in the y-direction near the centerline, for simplicity, we assume $j = 1$, i.e., the effect of NWS ranges from the wall to the centerline. Consequently, the volume size $V(i)$ is simply expressed as

$$V(i) \;=\; (h - \triangle y)(\triangle x)w, \tag{29}$$

where w is the width of the channel plate when $V(i)$ is 3-D.

The pressure difference in the y-direction is approximated by the mean difference between $x(i)$ and $x(i+1)$,

$$\triangle p(i) \;=\; \frac{1}{2}\left\{ p_{i,1} \;+\; p_{i+1,1} \right\} \;-\; \frac{1}{4}\left\{ p_{i,J0} \;+\; p_{i,J1} \;+\; p_{i+1,J0} \;+\; p_{i+1,J1} \right\} \tag{30}$$

Next, consider the elapsed time $\triangle t$ during which NWS acts on the flow passing along vorticities $\omega_{i,J0}$ and $\omega_{i+1,J0}$. The distance between $x(i)$ and $x(i+1)$ is $\triangle x$. The velocities at two points $(i, J1)$ and $(i+1, J1)$ are $u_{i,J1}$ and $u_{i+1,J1}$, respectively. Accordingly, the
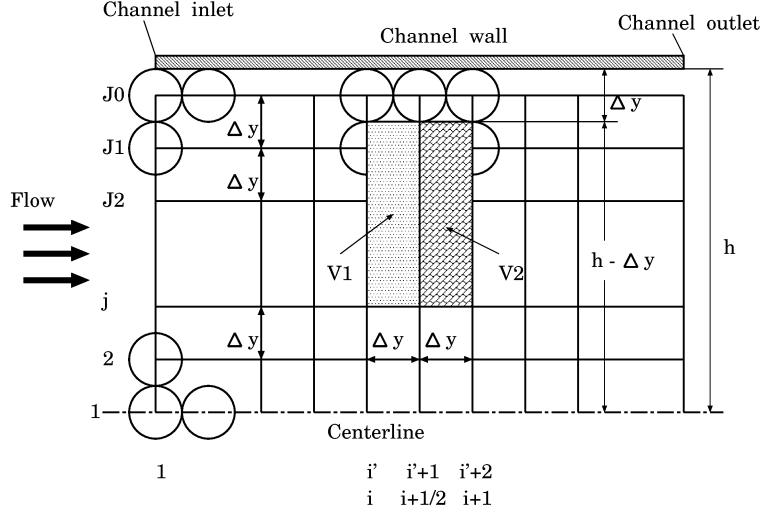
Figure 9: Mesh system, $\triangle x = \triangle y$.

elapsed time $\triangle t^*(i)$ may be given by dividing the axial grid space $\triangle x$ by the mean velocity at $j = J1$.

$$\triangle t^*(i) \;\equiv\; \frac{\triangle x}{\frac{1}{2}\left\{u_{i,J1} + u_{i+1,J1}\right\}} \;\approx\; \frac{\triangle x}{u_{i+1/2,J1}} \tag{31}$$

However, if this $\triangle t^*(i)$ is the correct period, the following inconsistency will be encountered. Two simple cases, (a) and (b), are taken as examples. In case (a), the mesh aspect ratio is $\triangle x = 2\triangle y$, as shown in Fig. 9, where $V1 = V2, V1 + V2 = V, i = i', i + 1/2 = i' + 1$, and $i + 1 = i' + 2$. The work $W(a)$ and the power $PW(a)$, for the shadowed space $(V1 + V2)$ between $x(i)$ and $x(i+1)$, respectively, are expressed as

$$W(a) \;=\; V\triangle p, \tag{32}$$

$$PW(a) \;=\; \frac{V\triangle p}{\dfrac{\triangle x}{u_{i+1/2,J1}}} \;=\; \frac{(V\triangle p)\,u_{i+1/2,J1}}{2\triangle y}. \tag{33}$$

Then, if the mesh aspect ratio is $\triangle x = \triangle y$, the work $W(b)$ in V is calculated by adding work in $V1$ and work in $V2$:

$$W(b) \;=\; V1\triangle p1 \;+\; V2\triangle p2 \;\approx\; V\triangle p. \tag{34}$$
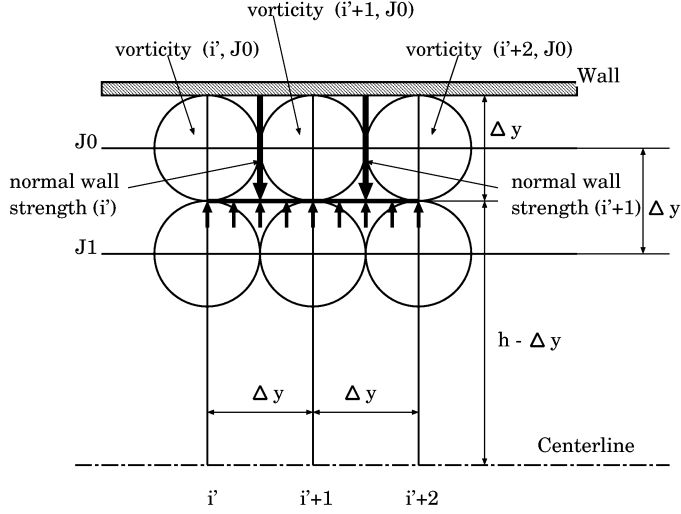
14

Figure 10: Balance of NWS and pressure at wall.

Similarly, the power $PW(b)$ in V is calculated by adding the powers in $V1$ and $V2$:

$$PW(b) = \underbrace{\frac{V1\triangle p1}{\triangle y}}_{u_{i'+1/2,J1}} + \underbrace{\frac{V2\triangle p2}{\triangle y}}_{u_{i'+3/2,J1}} \approx \frac{(V\triangle p)\,u_{i'+1,J1}}{\triangle y} \approx 2PW(a), \qquad (35)$$

where it is assumed that $\triangle p1 \approx \triangle p2 \approx \triangle p$ and $u_{i'+1/2,J1} \approx u_{i'+1,J1} \approx u_{i'+3/2,J1}$. Since $W(a)$ and $W(b)$ must be the same for the same volume V, PW must also be the same for the same volume V. On comparing $PW(a)$ and $PW(b)$, however, $PW(b)$ is twice as high as $PW(a)$. To avoid this inconsistency, the following elapsed time is required for a general mesh system of $\triangle x = n\triangle y$ (n = 1, 2, 3, ...):

$$\triangle t(i) \equiv \frac{\triangle y}{\frac{1}{2}\left\{u_{i,J1} + u_{i+1,J1}\right\}} = \frac{1}{\frac{1}{2}\left\{\frac{u_{i,J1}}{\triangle y} + \frac{u_{i+1,J1}}{\triangle y}\right\}} \approx \frac{1}{\frac{1}{2}\left\{\omega_{i,J0} + \omega_{i+1,J0}\right\}}, \qquad (36)$$

where the vorticity at the wall is approximated by Eq. (23).

NWS causes the pressure gradient in the y-direction. Figure 10 shows the balance of NWS and pressure at the contact surface of $j = 0.5(J0 + J1)$. The elapsed time given by Eq. (36) is based on the following assumptions.

(i) The no-slip condition at the wall means that the fluid particles are not translating; however, they are undergoing rotation. It can be imagined that the wall consists of an array of marbles which are rotating but remain at the same location at the wall $J = J0$ [15b].
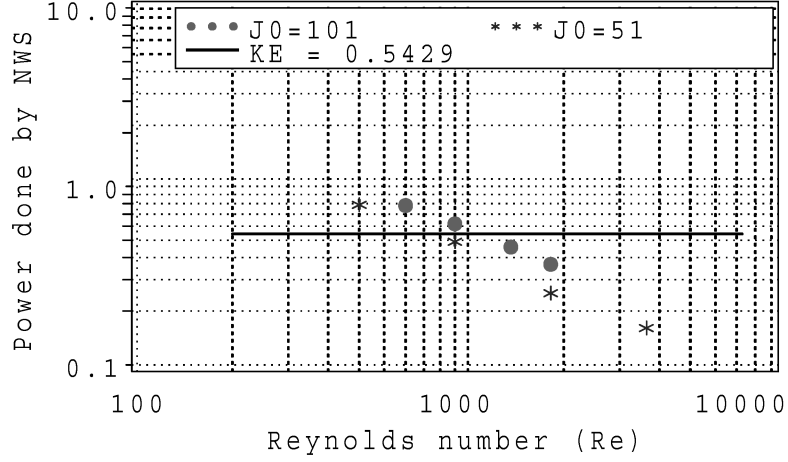
15

Figure 11: PW done by NWS for straight channel flow.

(ii) Rotation of a fluid particle at the wall yields a vortex and a vorticity. Then the curl of vorticity yields NWS, according to Eq. (15). The diameter of the vortex of the fluid particle on the wall is $\triangle y$. Accordingly, NWS is produced per vortex, or per $\triangle y$.

(iii) Since NWS is generated between adjacent vorticities, the effective distance in the x-direction which NWS affects is $\triangle y$, not $\triangle x$. This statement is confirmed using Eq. (37) in discrete form. Let $\triangle x$ be $n\triangle y$, then

$$\frac{\triangle p}{\triangle y} = \frac{2}{Re}\frac{\triangle \omega}{\triangle x} = \frac{2}{Re}\frac{\omega_{i+1} - \omega_i}{\triangle x} = \frac{2}{Re}\frac{\omega_{i'+n} - \omega_{i'}}{n\triangle y}$$

$$= \frac{2}{Re}\frac{1}{n\triangle y}\Big[\{\omega_{i'+n} - \omega_{i'+n-1}\} + \{\omega_{i'+n-1} - \omega_{i'+n-2}\} + \cdots$$

$$+\{\omega_{i'+1} - \omega_{i'}\}\Big] \approx \frac{2}{Re}\frac{n\{\omega_{i'+1} - \omega_{i'}\}}{n\triangle y} = \frac{2}{Re}\frac{\omega_{i'+1} - \omega_{i'}}{\triangle y} \qquad (37)$$

where the vorticity gradient is assumed to be linear in a small space between $x(i)$ and $x(i+1)$, i.e., $\omega_{i'+n} - \omega_{i'+n-1} \approx \omega_{i'+n-1} - \omega_{i'+n-2} \approx \cdots \approx \omega_{i'+1} - \omega_{i'}$.

Thus the total power PW done by NWS is obtained in dimensionless form (drop w) as

$$PW = \sum_i \frac{V(i)\,\triangle p(i)}{\triangle t(i)} = \frac{1}{8}(h - \triangle y)\triangle x \sum_i \Big[2\{p_{i,1} + p_{i+1,1}\}$$

$$-\{p_{i,J0} + p_{i,J1} + p_{i+1,J0} + p_{i+1,J1}\}\Big] \times \Big\{\omega_{i,J0} + \omega_{i+1,J0}\Big\} \qquad (38)$$

The calculated results of PW are listed in Table 2, and plotted against the Reynolds number in Fig. 11, where the dots and asterisks denote the results for $J0 = 101$ and $J0 = 51$ grid points in the y-direction, respectively. It is clear from Fig. 11 that (i) PW decreases as Re increases and (ii) at $Re = 1300$, the value of PW is approximately from 0.5 to 0.6.

16

Therefore, we must find another variable which has values from 0.5 to 0.6 at $Re = 1300$. Because we state the variable beforehand, it is the increase in kinetic energy per second, or power, in the entrance region.

3.4   Increase in kinetic energy (KE)

In the entrance region, the velocity distribution changes from uniform at the inlet to parabolic at the entrance length. The magnitude of the increase in kinetic energy is considered below.

At the inlet, the velocity profile is uniform: $u(0, y) = U$. Let w be the channel width. For half the channel, the kinetic energy across the inlet is given by multiplying the flux by its kinetic energy,

$$\int_0^h wdy \cdot U \cdot (\frac{1}{2}\rho U^2) \;=\; \frac{1}{2}\rho U^3 w \int_0^h dy \;=\; \frac{1}{2}\rho h w U^3. \tag{39}$$

At the entrance length, the velocity has a parabolic distribution and is expressed as

$$u(y) \;=\; \frac{3}{2}U \left\{ 1 - (\frac{y}{h})^2 \right\}. \tag{40}$$

From Eq. (40), the kinetic energy at the entrance length is calculated as

$$\frac{1}{2}\rho w \int_0^h \left[\frac{3}{2}U \left\{ 1 - (\frac{y}{h})^2 \right\} \right]^3 dy \;=\; \frac{27}{35}\rho h w U^3. \tag{41}$$

Accordingly, the increase in kinetic energy in the entrance region is obtained by subtracting Eq. (39) from Eq. (41).

$$\frac{27}{35}\rho h w U^3 \;-\; \frac{1}{2}\rho h w U^3 \;=\; \frac{19}{70}\rho h w U^3 \tag{42}$$

The dimensions of this increase in kinetic energy are

$$\left[\frac{kg}{m^3} \; m^2 \; (\frac{m}{sec})^3 \;=\; kg \; \frac{m^2}{sec^3} \;=\; kg \; \frac{m}{sec^2} \; \frac{m}{sec} \right].$$

Note that this unit corresponds to power in physics, i.e., energy per second. We define the dimensionless increase in kinetic energy per second, or acceleration power, KE, as

$$KE \;\equiv\; \frac{\frac{19}{70}\rho h w U^3}{\frac{1}{2}\rho h w U^3} \;=\; \frac{19}{35} \;=\; 0.5429. \tag{43}$$

This value of 0.5429 for channel flow is constant regardless of Re.

3.5 Calculation of $Rc(min)$

The minimum critical Reynolds number $Rc(min)$ is calculated via linear interpolation. In the case of $J0 = 101$, employing the values of PW for $Re = 1000$ and 1500,

$$\frac{Rc(min) - 1000}{0.5429 - 0.6167} = \frac{1500 - 1000}{0.4582 - 0.6167}. \tag{44}$$

From Eq. (44), we obtain $Rc(min) \approx 1230$.
In the case of $J0 = 51$, employing the values of PW for $Re = 500$ and 1000,

$$\frac{Rc(min) - 500}{0.5429 - 0.7906} = \frac{1000 - 500}{0.4905 - 0.7906}. \tag{45}$$

From Eq. (45), we obtain $Rc(min) \approx 910$.

$Rc(min) = 1230$ is much closer to the experimental value of 1300 than the approximate value of 7700 given by the stability theory.

4 Conclusions

From previous experiments performed under the conditions of natural disturbances, it is clear that (i) the laminar-turbulent transition occurs in the entrance region and (ii) Rc takes a minimum value, $Rc(min)$, when using a straight pipe or a straight channel, i.e., no bellmouth is fitted at the inlet. On the basis of this knowledge, we proposed the laminar-turbulent transition model. The following conclusions were obtained in the present study.
(1) The transition model was verified by determining $Rc(min)$ for channel flow. The calculated results of $Rc(min)$ were 1230 when using $J0 = 101$ grid points in the y-direction and 910 when $J0 = 51$.
(2) In the entrance region, there exist two parameters, i.e., the increase in kinetic energy per second (KE) and the power (PW) done by NWS. For the dimensionless $X(= x'/HRe)$ coordinate, KE is constant regardless of Re, but PW varies approximately inversely with Re. The intersection point of two lines of the two parameters indicates the value of $Rc(min)$.

The proposed model is a hypothetical macromodel and does not represent the fine structure of turbulence well. The calculated values of $Rc(min)$, however, were close to the experimental values for both pipe and channel flows. Therefore, we cannot ignore the model and must further calculate $Rc(min)$ and $Rc2(BD/D, min)$ for flows in bellmouth entrances using more refined meshes such as $\triangle X = 0.00001$ to obtain the true values of $Rc(min)$ and $Rc2(BD/D, min)$. Moreover, we must further study the relationship between the pressure difference in the y-direction and the excess pressure drop $K(X)$; The pressure difference decreases inversely with Re, while $K(X)$ is constant regardless of Re for the X coordinate.

5 Acknowledgment

References

[1] Reynolds, O., *Trans. Roy. Soc. Lond.*, **174** (1883), 935-982.

[2] Lamb, H., *Hydrodynamics (6th ed.)*, (Cambridge University Press, 1975), 664-665.

[3] Tatsumi, T., *J. Phy. Soc. of Japan*, **7** (1952), 489-502.

[4] Huang, L. M. and Chen, T. S., *J. Fluid Mech.*, **63** (1974), 183-193.

[5] Goldstein, S., *Modern Developments in Fluid Dynamics, Vol. I*, (Dover, 1965), 299 and 97.

[6] Chen, R-Y., *Trans. of ASME, J. of Fluids Eng.*, (March 1973), 153-158.

[7] Kanda, H., *Proc. of ASME Fluids Engineering Division*, FED-Vol. **250** (1999), 189-196.

[8] Kanda, H., *Proc. of ASME Fluids Engineering Division*, FED-Vol. **250** (1999), 197-204.

[9] Wang, Y. L. and Longwell, P. A., *A.I.Ch.E. Journal*, **10, No. 3** (1964), 323-329.

[10] Morihara, H. and Cheng, R. T., *J. Comput. Phys.*, **11** (1973), 550-572.

[11] Davies, S. J. and White, C. M., *Proc. of Royal Society*, **A119** (1928), 92–107.

[12] Patel, V. C. and Head, M. R., *J. Fluid Mech.*, **38, part 1** (1969), 181-201.

[13] Drazin, P. G. and Reid, W. H., *Hydrodynamic Stability*, (Cambridge University Press, 1981), 223.

[14] Kanda, H., *Proc. of ASME Fluids Engineering Division*, IMECE2005-80637, (2005).

[15] Prandtl, L. and Tietjens, O.G., *Applied Hydro- and Aeromechanics*, (Dover, 1957), 35.

[16] Rivas, M. A. and Shapiro, A.H., *Trans. of ASME*, (April 1956), 489-497.

[17] Wygnanski, I. J. and Champagne, F. H., *J. of Fluid Mech.*, **59, part2** (1973), 281-335.

[18] Panton, R. L., *Incompressible Flow*, (Wiley-Interscience, 1984), 377 and 323.

[19] Roache, P. J., *Fundamentals of Computational Fluid Dynamics*, (hermosa, Albuquerque, 1998), 199.

[20] White, F. M., *Fluid Mechanics (4th ed.)*, (McGraw-Hill, 1999), 260.

[21] Bodoia, J. R. and Osterle, J. F. *Appl. Sci. Res. Section A*, **10** (1961), 265-276.

[22] Kiya, M., Fukusako, S., and Arie, M., *Bulletin of JSME*, **15, No. 81** (1972), 324-336.

[23] Kanda, H., *Proc. of ASME Fluids Engineering Division*, FED-Vol. **256** (2001), 189-196.

[24] Kondepudi, D. and Prigogine, I., *Modern Thermodynamics*, (John Wiley & Sons, 1998), 56.